

Spherulite Nucleation in Blends of Isotactic Polypropylene with Isotactic Poly(butene-1)

Z. BARTCZAK,^{1*} A. GALESKI,¹ and M. PRACELLA²

¹Centre of Molecular and Macromolecular Studies, Polish Academy of Sciences, 90 362 Łódź, Poland, and ²Centro Studi Processi Ionici di Polimerizzazione, CNR, 56 100 Pisa, Italy

SYNOPSIS

The phase morphology and the influence of composition on the primary nucleation of isotactic polypropylene in isotactic polypropylene/isotactic poly(butene-1) (iPP/iPB) blends were investigated by electron and light microscopy and small-angle light scattering. It was found that iPP and iPB are miscible but the thermal treatment induces partial phase separation of components and the formation of iPP-rich and iPB-rich phases. The complete phase separation needs high temperatures and/or a long time of melt annealing. In samples crystallized isothermally at low undercooling the heterogeneous primary nucleation in blends is depressed as compared to plain iPP. In blends the less active heterogeneities lose their activity because of an increase of the energy barrier for critical size nucleus formation due to phase separation of blend components during crystallization. For the same reason the rate of homogeneous nucleation in blends decreases, as observed in samples crystallized at very high undercooling. At very high undercooling iPP and iPB are able to crystallize with similar rates, which results in the formation of a fraction of iPB spherulites in addition to iPP spherulites. Consequently the number of spherulites in the blend is larger than that in plain iPP, in spite of the decrease in the homogeneous nucleation rate of iPP in the blend. © 1994 John Wiley & Sons, Inc.

INTRODUCTION

Among many polymer blends the polyolefin blends are of high importance because of a combination of useful engineering properties, low cost–performance ratio, and low energy consumption for production. Thus, polyolefin blends, especially those based on isotactic polypropylene (iPP), have been intensively investigated in recent years.

Numerous studies have shown that mechanical properties of crystalline polymers depend strongly on their morphology. Because the failure is frequently initiated at interspherulitic boundaries (see e.g., Ref. 1), the primary nucleation process that controls the spherulite size appears to be very important for mechanical properties of semicrystalline polymers.

In previous work we reported studies on the primary nucleation in incompatible iPP-based blends.^{2–5} We found that primary nucleation of iPP spherulites in those blends strongly depends on the type of the second polymer. It was shown that the main reason for the changes in primary nucleation behavior is the phenomenon of migration of heterogeneities (as solid impurities, additives, etc.) constituting potential heterogeneous nuclei from one blend component to the other during the melt-mixing process. The driving force for the migration is the difference between the surface free energies of those heterogeneities with respect to both molten blend components. The limited miscibility of the components also affects the primary nucleation process.⁴

The goal of investigations reported here was to extend the study of spherulite nucleation in polyolefin based blends to miscible systems. Isotactic polypropylene and isotactic poly(butene-1) (iPB) were chosen because of reported miscibility of blend components^{6,7} and the technological importance of their blends. Morphology, properties, and prepara-

* To whom correspondence should be addressed.

tion of blends of iPP with iPB were previously investigated by several authors.⁶⁻¹¹ It was reported that both polymers are miscible in any proportions in the molten state.^{6,7} Piloz et al.⁷ found single T_g values for iPP/iPB blends at a temperatures between the T_g for homopolymers. In general, iPP and iPB crystallize separately,^{8,9} although the cocrystallization was also reported for very high cooling rates.¹⁰ It was found that iPP in blends with iPB can act as a nucleating agent for the crystallization of iPB from the molten state and accelerates the transformation of the iPB crystal form II to the form I.¹¹ On the other hand, the presence of iPB in the blend influences the crystallization of iPP: both the spherulite growth rate and overall crystallization rate decrease with increasing concentration of iPB in the blend.⁹

This work reports the study of the phase behavior and primary nucleation of iPP in iPP/iPB blends. The investigations of primary nucleation were carried out in a broad range of crystallization temperatures in order to study the influence of iPB on both heterogeneous and homogeneous modes of primary nucleation of crystallization of iPP in molten iPP/iPB blend.

EXPERIMENTAL

Materials and Blend Preparation

The polymers employed were isotactic polypropylene (RAPRA, $M_w = 3.07 \times 10^5$, $M_n = 1.56 \times 10^4$, density 0.906 g/cm^3 , melt flow index 3.9 g/10 min) and isotactic poly(butene-1) (PETROTEX, $M_w = 1.06 \times 10^6$, $M_n = 6.3 \times 10^4$, $M_w/M_n = 16$ [evaluated by gel permeation chromatography (GPC) in trichlorobenzene at 135°C]).

Blends containing 0, 10, 30, and 50 wt % iPB were prepared by melt mixing of components in the desired proportions at 190°C using a laboratory mini-extruder (Custom Sci. Inc.). The blending of polymers was repeated twice for each composition.

Morphological Observations

The phase structure of the blend samples was investigated by transmission (TEM) and scanning electron microscopy (SEM). The microscopes used were the Tesla BS500 (TEM) and Jeol JSM-T300 (SEM). Samples of iPP and iPP/iPB blend destined for microscopic observations were melt annealed at a temperature of 170, 190, or 220°C for various periods of time (5–30 min) and then crystallized isothermally at 125°C . Then their surfaces were etched

with permanganic etchant according to the method of Olley and Basset.¹² For TEM observations two-stage carbon replicas were prepared from the etched sample surface. The same etched samples were observed directly using a scanning electron microscope (coating with gold was used prior to observations).

Crystallization at Low Undercooling

In order to study the heterogeneous nucleation mode, crystallization of blends at low and moderate undercooling was performed. Samples in the form of 10–20- μm -thick films were obtained by sectioning the extrudates with an ultramicrotome (Tesla BS 490A) and sandwiching them between microscope cover glasses. Prior to crystallization the samples were melted and annealed at 220°C for 5 min in order to destroy the self-seeded nuclei. During preparation any accidental shear or flow of the molten samples was carefully avoided. The samples were further crystallized isothermally on a microscope hot stage connected to the temperature control unit. The temperature of the hot stage was maintained with an accuracy better than 0.1°C . Isothermal crystallizations were conducted at several temperatures in the range of 119 – 130°C . Sample thickness, necessary in calculations of nucleation density, was measured with an accuracy of better than $1 \mu\text{m}$. Primary nucleation of spherulites in isothermally crystallized samples was studied by polarized microscopy. The number of spherulites was determined after completion of crystallization and recalculated to the number of primary nuclei per volume unit of the blend and/or per volume unit of iPP in the blend (the nucleation density D). The error of estimation of nucleation density was less than 5%.

The spherulite size distributions were determined from the micrographs of completely crystallized samples. The micrographs were cut along the interspherulitic boundaries and then each fragment of a micrograph, representing a single spherulite was weighed in order to calculate the occupied area. On the basis of the spherulite area its average radius was calculated. The population of spherulites considered was in the range of 200–400 for each sample.

Nonisothermal crystallizations of the samples with cooling rates from 1.25 to 20°C/min were carried out by differential scanning calorimetry (DSC) using the Perkin-Elmer DSC-2B apparatus.

Crystallization at High Undercooling

Isothermal crystallization in the temperature range 67 – 82°C was carried out applying a different pro-

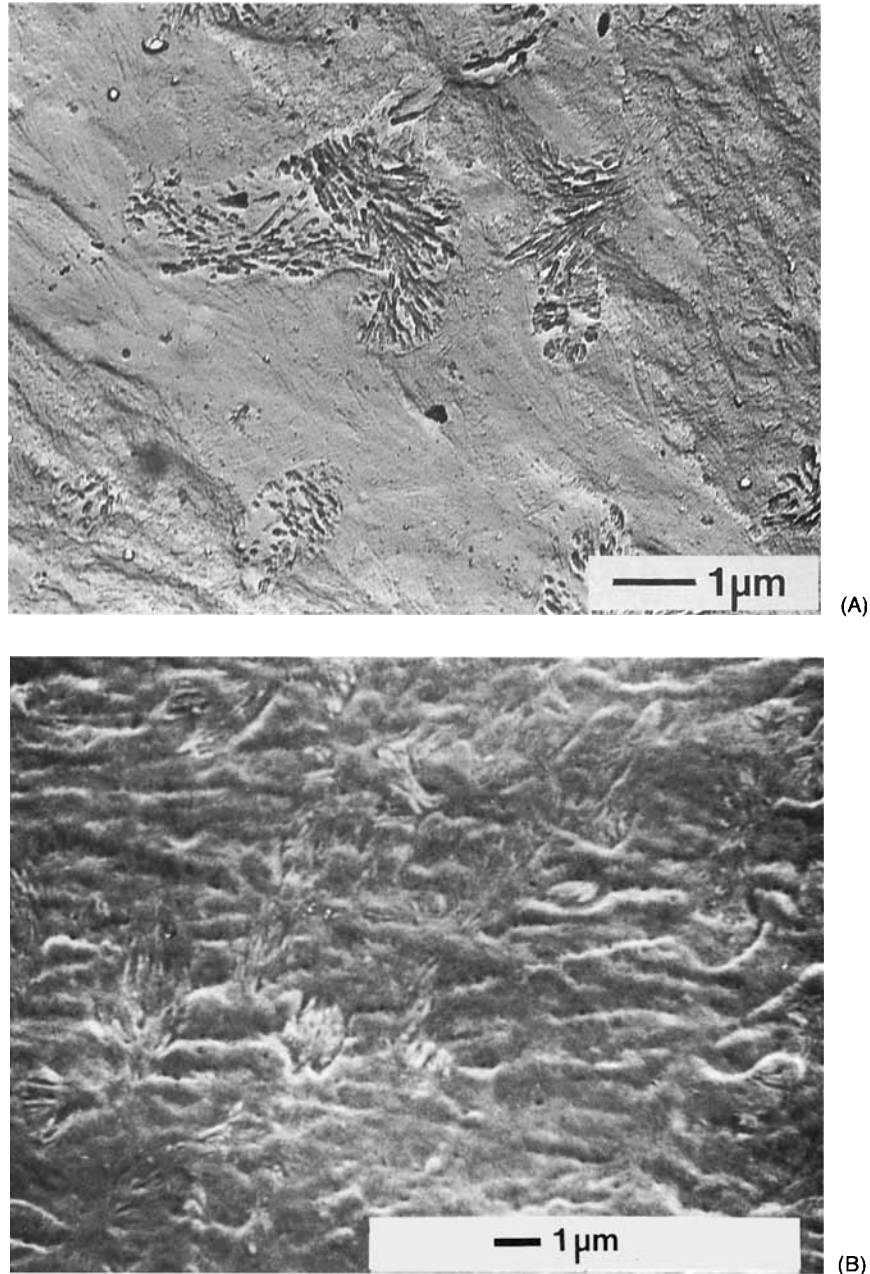


Figure 1 Electron micrographs of etched surface of 7 : 3 iPP/iPB blend. Sample was crystallized nonisothermally after melting at 190°C for 5 min. (a) Transmission electron micrograph of surface replica; (b) scanning electron micrograph of surface.

cedure. Samples in the form of films that were approximately 20 μm thick were sandwiched together, with a 20- μm -thick aluminum frame used as a spacer, between two 5- μm -thick aluminum foils, and then melted in a laboratory press for 5 min at a temperature of 190°C and pressure of 50 atm. Then the samples were quickly transferred to the crystallization cell, the temperature of which was electronically controlled with an accuracy of $\pm 0.01^\circ\text{C}$.

The crystallization cell consisted of two cylindrical blocks made from aluminum, both having mass approximately equal to 5 kg, equipped with electrical heaters and platinum resistance thermometers connected to the temperature controller.^{13,14} The sandwiched sample was placed between blocks. The block faces were finely polished and the blocks were pressed firmly together in order to improve the thermal contacts between the sample and the blocks.

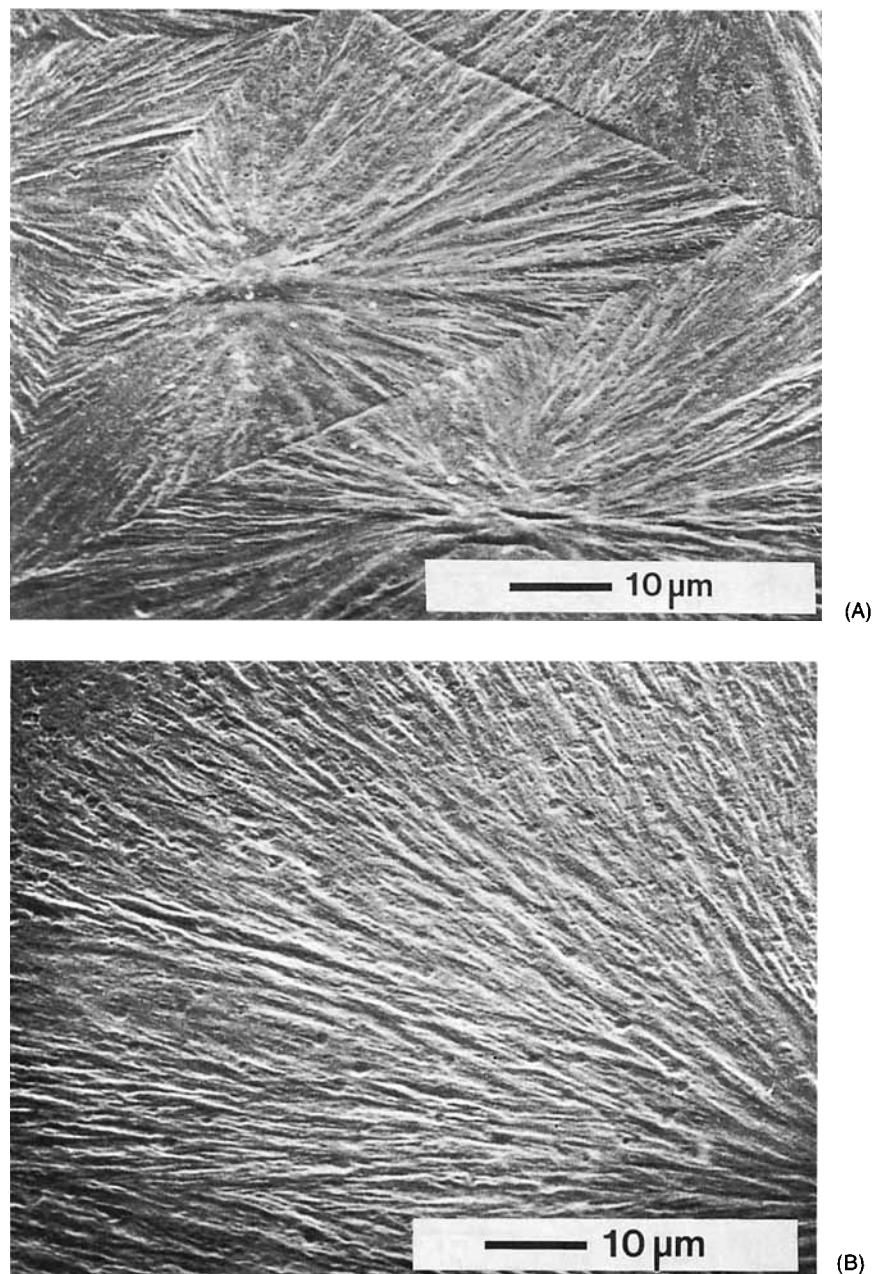


Figure 2 Scanning electron micrographs of etched surfaces of samples of iPP/iPB blend melted at 190°C for 5 min and then crystallized isothermally at 125°C: (a) iPP; (b) 9 : 1 iPP/iPB; (c) 5 : 5 iPP/iPB.

Owing to the very small heat capacity of the sample (including the thin cover foil), the large heat capacity of the aluminum blocks, the precise control of their temperature, and good thermal contacts between the sample and the cell, it was possible to cool the sample down to the desired crystallization temperature very quickly. Isothermal conditions in the temperature range of 65–85°C were reached inside the sample volume in times shorter than 0.5 s after transferring

to the cell as determined by a thin thermocouple embedded in the sample. The equilibration time is more than one order of magnitude shorter than the estimated time needed for complete crystallization of iPP at those temperatures.¹⁴

The samples of blends containing 0–30 wt % of iPB were crystallized isothermally in the temperature range 67–82°C with an interval of 1°C. Crystallized samples were investigated by means of

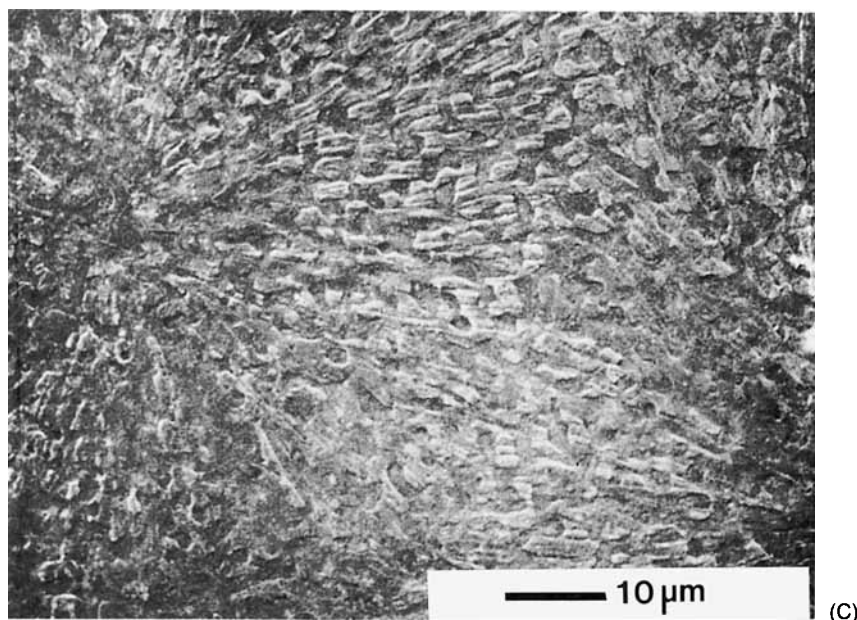


Figure 2 (Continued from the previous page)

small-angle light scattering (SALS) in order to determine the average spherulite radius from the H_v scattering pattern. He-Ne laser ($\lambda = 632.8$ nm) was used to generate the scattering patterns. The H_v intensity distribution was recorded using a photogoniometer.

For each blend composition and crystallization temperature three or more samples were crystallized and their H_v scattering intensity distributions were recorded. The absolute error on the determination of average spherulite radii did not exceed $0.5 \mu\text{m}$.

On the basis of the dependence of the average spherulite radius on the crystallization temperature, the instantaneous nucleation densities and the spontaneous nucleation rates were estimated. Details of the experimental procedure and the calculation principles have been described elsewhere.¹⁴

RESULTS AND DISCUSSION

Phase Morphology

Figure 1 presents two micrographs of the etched surface of 7 : 3 iPP/iPB blend melt annealed for 5 min prior to crystallization at 190°C . The micrograph in Figure 1(a), obtained using a transmission electron microscope and the shadowed carbon replica, demonstrates that iPP and iPB in a solid iPP/iPB blend are phase separated and crystallized with different morphology. The matrix exhibits the

“cross-hatched” lamellar morphology typical for iPP. The morphology of inclusions is different and similar to that observed for the iPB sample prepared under similar conditions. Figure 1(b) shows the SEM micrograph of the same sample. Although the resolution of this SEM micrograph is much lower than that of TEM micrographs, also on this micrograph the phase separation can be observed. Both micrographs shown in Figure 1 demonstrate clearly that iPP and iPB are not completely miscible and phase separation takes place in their blend. The shape, size, and position of iPB inclusions inside iPP spherulite demonstrate that phase separation has occurred before crystallization of iPP spherulites started. The above conclusion is in contradiction with the published results, suggesting complete miscibility of iPP and iPB.^{6,7} On the other hand, the blends obtained directly from the mixer and observed in an electron microscope gave the impression of a homogeneous system with no clear features of phase separation.

Figure 2 shows the SEM micrographs of iPP and iPP/iPB blends melt annealed at 190°C for 5 min prior to crystallization. In the micrographs of the blends (Figs. 2(b)–(c)) the phase separation of components can be easily observed. The number and size of the iPB inclusions increase with increasing content of iPB in the blend. However, the analysis of the micrographs demonstrated that the estimated total volume of the inclusions is smaller than the nominal amount of iPB in the blend, which suggest

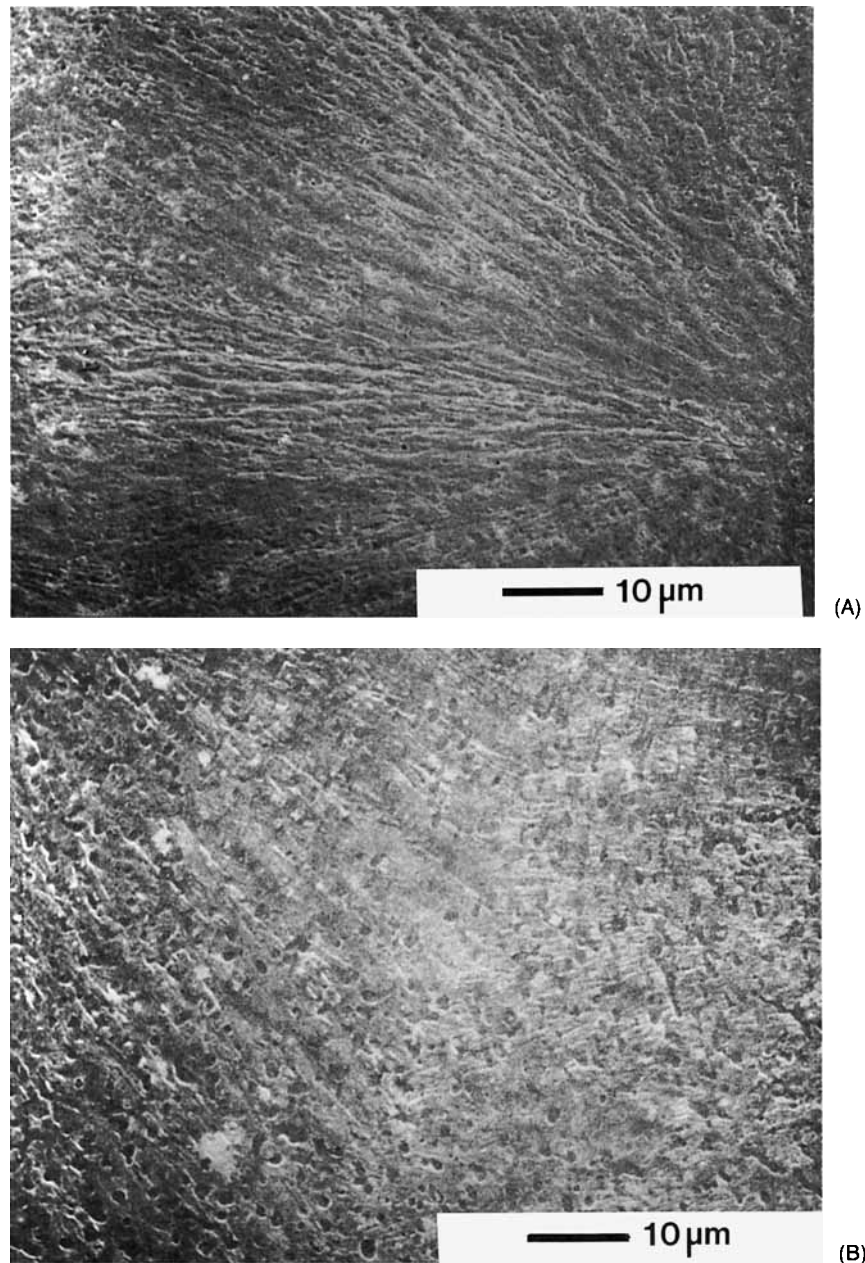


Figure 3 Scanning electron micrographs of etched surfaces of samples of 7 : 3 iPP/iPB blend crystallized isothermally at 125°C. The samples were melted prior to crystallization: (a) at 170°C, 5 min; (b) at 190°C, 5 min; (c) at 220°C, 5 min; (d) at 170°C, 30 min.

that the phase separation was not complete and thus the blend components remained partially mixed. Additional support for such a conclusion is given by the appearance of the interspherulite boundaries. The interspherulite boundary lines in plain iPP are sharp and well defined, whereas in blends they are very diffuse and frequently hard to distinguish [compare Figs. 2(a) and 2(c), showing iPP and 5 : 5

blend, respectively]. Such appearance of spherulite boundaries is probably a result of a coarsening of a growing front of spherulites due to local phase separation.

Figures 3(a)–(c) present the micrographs of the 7 : 3 blend samples melt annealed for 5 min at various temperatures prior to crystallization (170, 190, and 220°C, respectively). Figure 3(d) presents the

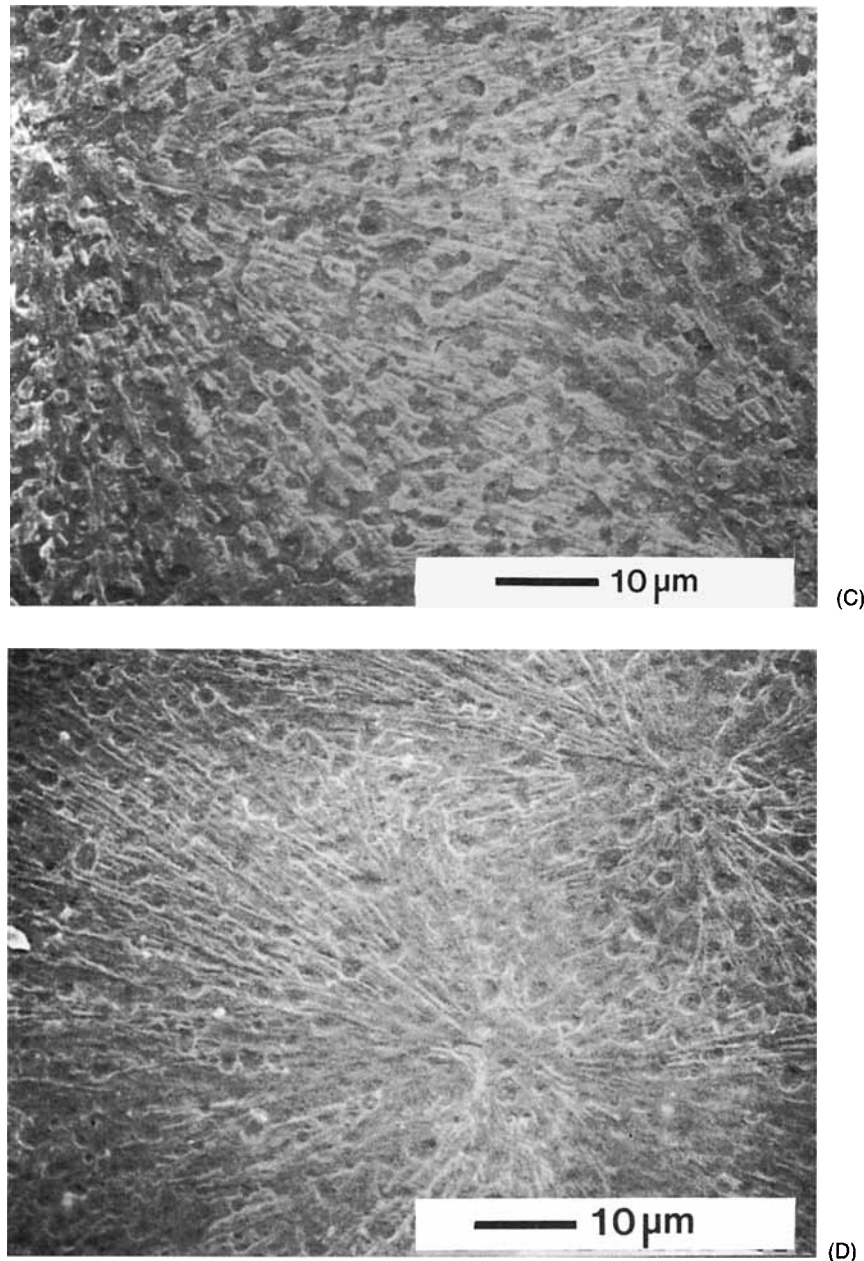


Figure 3 (Continued from the previous page)

micrograph of the sample of the same composition but melt annealed at 170°C for 30 min prior to crystallization. These photographs demonstrate that the phase separation of blend components intensifies with an increase of the temperature and/or time of melt annealing.

The reported observations suggest that iPP and iPB are miscible and can form a single phase under particular conditions, but such a phase structure is unstable on annealing. After melt mixing, a prac-

tically homogeneous structure is formed due to high shear forces. However, the prolonged melt annealing of iPP/iPB blends, in the absence of any shear, induces the phase separation of components. The complete separation of blend components needs a long time, thus under normal melting conditions (e.g., 200°C for a few minutes), the newly formed phases are still mixtures of both components: the matrix is an iPP-rich phase, while the inclusions constitute an iPB-rich phase.

Heterogeneous Nucleation of iPP (Low Undercooling for iPP)

For the crystallization conditions used ($T_m = 220^\circ\text{C}$, $T_c = 119\text{--}130^\circ\text{C}$) only the crystallization of iPP component nucleated on heterogeneous nuclei is possible. Homogeneous and self-seeded nucleation modes of iPP do not appear because of the relatively small undercooling and high temperature of melt annealing of the samples prior to crystallization, respectively.¹⁵ Crystallization of iPB occurs at much lower temperature than that used here.¹⁶

The noticeable decrease of the number of spherulites (i.e., primary nuclei) with an increase of iPB content was observed in blends. However, after recalculation of the nucleation density, defined as the number of primary nuclei per volume unit of iPP present in the blend (N/V), this decrease is much smaller. Figure 4 presents the nucleation densities in blends plotted against blend composition for various crystallization temperatures. It is seen that the nucleation density in blends decreases slightly with increasing iPB content. This decrease is more pronounced at lower crystallization temperatures than at higher ones. At 130°C the nucleation density is practically independent of the blend composition. Such a result demonstrates that iPB component incorporated in the blend does not influence markedly the nucleation process of iPP and the decrease of the number of spherulites observed in blends is mainly a concentration effect. The influence of iPB on heterogeneous nucleation of iPP is much weaker than in other polypropylene-based blends.²⁻⁵

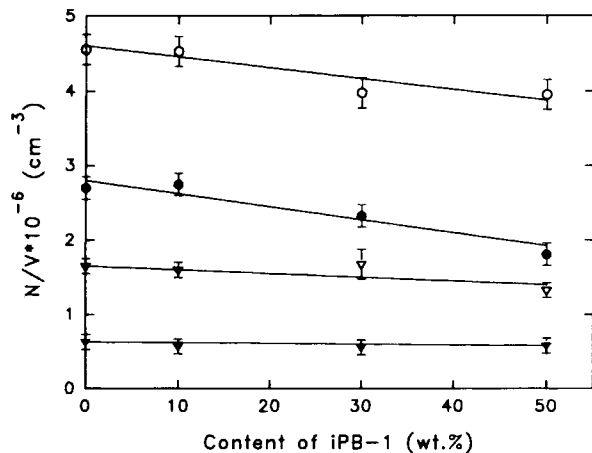


Figure 4 Dependence of number of primary nuclei per volume unit of iPP in blends of iPP with iPB on composition. Crystallization temperatures: (○) 119°C , (●) 123°C , (▽) 125°C , (▼) 130°C .

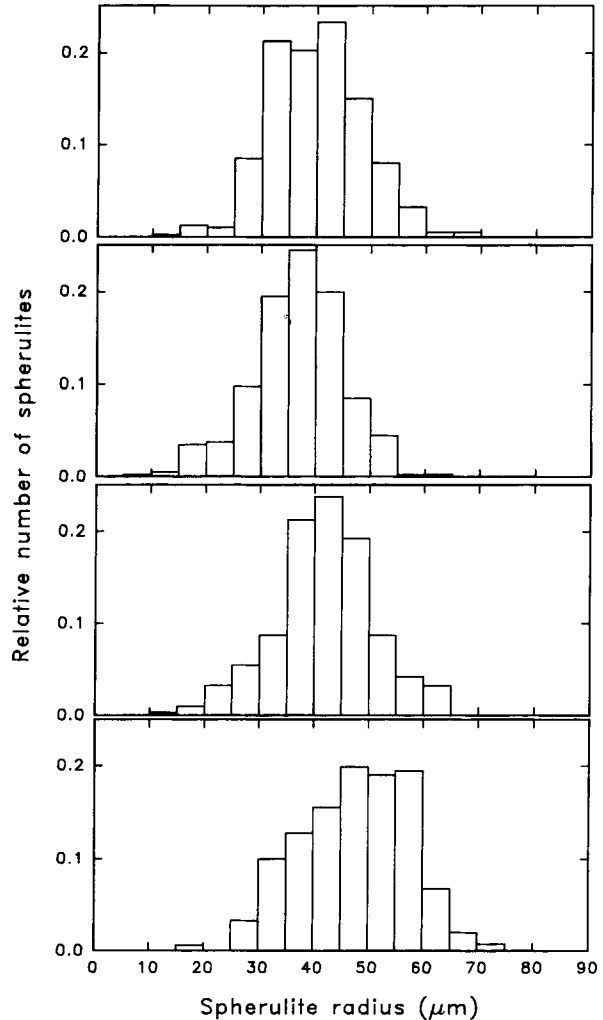


Figure 5 Spherulite size distributions in samples crystallized isothermally at 119°C : (a) iPP; (b) 9 : 1 iPP/iPB; (c) 7 : 3 iPP/iPB; (d) 5 : 5 iPP/iPB.

It is known^{17,18} that the distribution of spherulite sizes depends on the mode of primary nucleation. The shape of that distribution for instantaneous nucleation is similar to the shape of the error function. In the case of mixed instantaneous-spontaneous nucleation the distribution broadens markedly with increasing contribution of spontaneous nuclei. Thus, the examination of the shape of the spherulite size distribution can deliver information on the character of the primary nuclei active in the crystallization process. Figure 5 presents the spherulite size distributions determined for samples of blends crystallized at 119°C . The distribution shape for a plain iPP sample indicates mixed instantaneous-spontaneous type of nucleation. In blends with the content of iPB increasing up to 30 wt %, the distri-

bution narrows, which suggests a change of character of the nucleation process toward instantaneous nucleation. In the 5 : 5 blend the nucleation retrieves its mixed character.

The spherulite size distributions for samples crystallized at 125°C (not shown here) do not differ markedly one from another. This confirms that the nucleation behavior of iPP in iPP/iPB blends at higher crystallization temperatures is less affected by the presence of iPB.

The changes in the shape of spherulite size distributions observed in blends crystallized at 119°C are entirely the result of changes to a heterogeneous nucleation mode (homogeneous and self-seeding nucleation modes are unlikely to occur). The heterogeneous nuclei usually have a broad spectrum of activity: some of them are highly active and able to cause instantaneous nucleation of iPP, even at high crystallization temperatures, whereas the less active ones appear to be spontaneous or are inactive at a given crystallization temperature. As a result the spherulite size distribution for plain iPP has the shape characteristic for mixed type of nucleation. In the iPP/iPB blends the presence of iPB, partially miscible with iPP, suppresses the activity of heterogeneities as nucleation centers probably due to an increase of the energy barrier for the formation of a critical nucleus. However, that influence is rather weak, as demonstrated by the nucleation density data shown in Figure 4. Consequently, most heterogeneities, which would be active in plain iPP, retain their activity also in blends with low or moderate content of iPB; the less active heterogeneities assume a spontaneous character while the weakest potential nuclei lose their activity at a given temperature. Hence, at 119°C the number of spontaneous nuclei in the blends decreases as compared to plain iPP and the character of primary nucleation in blends changes toward instantaneous. At higher crystallization temperatures (e.g., 125°C) less active nuclei are already excluded from the crystallization process due to thermal conditions in both plain iPP

Table I Relative Densities of Nucleation of iPP Spherulites in iPP/iPB Blends by Ratio D/D_{130}

Temperature of Crystallization (°C)	10 : 0	9 : 1	7 : 3	5 : 5
130	1	1	1	1
125	2.62	2.43	2.81	2.16
123	4.25	4.33	4.05	2.81
119	6.85	6.66	6.50	6.42

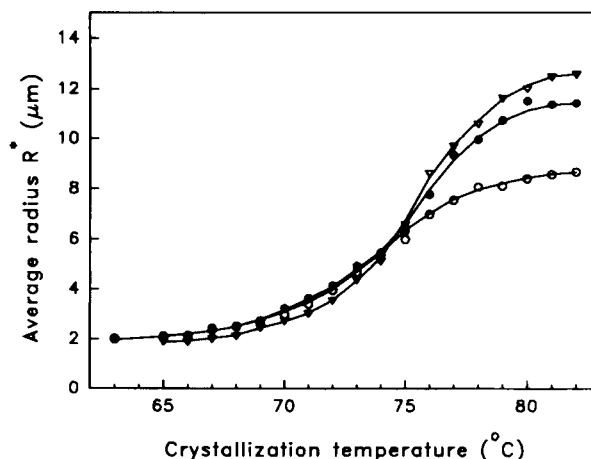


Figure 6 SALS determined average spherulite radius plotted as function of crystallization temperature: (○) iPP, (●) 9 : 1 iPP/iPB, (▽) 7 : 3 iPP/iPB.

and the blend; only highly active heterogeneities are able to nucleate at this temperature. The influence of iPB in the blend is too weak to depress markedly their activity, thus the nucleation process in the blend practically does not differ from that in plain iPP. Support for the above explanation is given in the Table I, where the ratios of the number of primary nuclei active at a given temperature to the number of highly active nuclei (active at 130°C) are presented. These data show that the relative number of nuclei active at low temperature decreases with increasing concentration of iPB in the blend. The activity of less active heterogeneities is depressed more than those having high activity. Such a conclusion is in agreement with the discussed changes of spherulite size distribution for samples crystallized at 119°C.

Nucleation at Low Crystallization Temperature

In the second set of experiments we investigated the primary nucleation of iPP spherulites in iPP/iPB blends crystallized at very low crystallization temperatures ranging from 67 to 82°C (undercooling for iPP larger than 100°C). It is known that in this temperature range the homogeneous primary nucleation of plain iPP is reached.^{19,20}

Figure 6 presents the dependencies of average spherulite radius R^* on the crystallization temperature T_c for plain iPP and for blends with iPB. The radii R^* were estimated from SALS of completely crystallized samples according to Stein's theory²¹:

$$R^* = \frac{4.09}{4\lambda \sin(\theta_m/2)} \quad (1)$$

where λ is the wavelength of the incident light and θ_m is the radial angle at which the maximum of the intensity in the H_v light-scattering pattern occurs.

It was demonstrated¹⁴ that it is possible to estimate the density of instantaneous nucleation D_i and the ratio of the sporadic nucleation rate I_s to the spherulite growth rate G from the dependence of SALS average spherulite radius R^* on the temperature of crystallization T_c by fitting theoretical curves R^* vs. T_c to the experimental data. For the purpose of those calculations the average spherulite radius was calculated from the distance distribution of boundary points to the center of the spherulite, $p_3(r)$, using the following formula^{14,22}:

$$R^* = \frac{\langle R^n \rangle}{\langle R^{n-1} \rangle} = \frac{\int_0^\infty r^n p_3(r) dr}{\int_0^\infty r^{n-1} p_3(r) dr} \quad (2)$$

where n is the order of averaging ($n = 5$ for three-dimensional spherulite growth¹⁴) and

$$p_3(r) = 4\pi r^2 \left(4\pi D_i^2 r^2 + 4\pi \frac{D_i I_s}{3 G} r^3 + \frac{I_s}{G} \right) \times \exp \left[-\frac{4}{3} \pi r^3 \left(D_i + \frac{r I_s}{4 G} \right) \right] \quad (3)$$

At high undercooling practically all heterogeneous nuclei are instantaneous in character, whereas homogeneous nuclei appear always to be sporadic. Thus the quantities D_i and I_s in Eq. (3) may be replaced by the density of heterogeneous nucleation D and the rate of homogeneous nucleation I , respectively. At very high undercooling all heterogeneities are active, so the nucleation density does not depend on temperature and can be represented by a constant during calculations. On the other hand, the rate of homogeneous nucleation I and the spherulite growth rate G are functions of the temperature of crystallization, which can be expressed by following equations^{23,24}:

$$I = I_0 \exp \frac{-\Delta F^*}{kT} \exp \frac{-32\sigma^2\sigma_e}{\Delta g_f^2} \quad (4)$$

and

$$G = G_0 \exp \frac{-\Delta F^*}{kT} \exp \frac{-4b_0\sigma\sigma_e}{\Delta g_f} \quad (5)$$

Hence

$$\frac{I_s}{G} = \frac{I}{G} = \frac{I_0}{G_0} \frac{\exp(-32\sigma^2\sigma_e/\Delta g_f^2)}{\exp(-4b_0\sigma\sigma_e/\Delta g_f)} \quad (6)$$

In the above equations I_0 and G_0 are constants, ΔF^* is the activation free enthalpy of diffusion of crystallizing elements across the liquid-crystal interface, σ and σ_e are lateral and fold surface free energies of the crystal, and Δg_f is the free enthalpy of fusion depending on the temperature of crystallization. The use of Eq. (5) in the form appropriate for regime III of crystal growth²⁴ is justified for temperatures in the investigated range. All parameters present in the Eqs. (4)–(6) are known for iPP^{23,24}; thus I/G can be calculated. Substitution of Eqs. (3) and (6) into Eq. (2) leads to the expression for the average spherulite radius as a function of the temperature of crystallization T_c [through $\Delta g_f = f(T_c)$] with two parameters of primary nucleation (heterogeneous nucleation density D and homogeneous nucleation rate I_0). These two parameters can be found by the fit of the function R^* vs. T_c to the experimental data.

The calculations performed for plain iPP¹⁴ gave a value of the density of heterogeneous (instantaneous) nucleation of nearly 1×10^9 nuclei/cm³ and homogeneous (sporadic) nucleation rate constant $I_0 = 9.5 \times 10^{35}$ cm⁻³ s⁻¹ (which is in fair agreement with the value 10^{34} predicted theoretically²³). Moreover, those calculations led to the conclusion that the average spherulite radius in iPP is controlled mainly by the heterogeneous primary nucleation at T_c above 80°C, because the rate of homogeneous nucleation is still relatively low at those temperatures, and by homogeneous nucleations below 76–77°C. At intermediate crystallization temperatures both nucleation modes compete.

The rates of homogeneous nucleation and spherulite growth in a miscible blend (completely or partially) are different than those in a plain crystallizing component. Such differences result from modified conditions for otherwise the same process of crystallization. Thus, both primary nucleation and crystal growth can be described by equations of the form of Eqs. (4) and (5). The differences manifest in (i) modification of activation free enthalpy of diffusion ΔF^* , which reflects different conditions for transport of the crystallizing segment in molten plain polymer than in a mixture, and (ii) modification of the free enthalpy of fusion, which should be increased in miscible blends by the free enthalpy of mixing: $\Delta g_f' = \Delta g_f + \Delta g_m$, because the crystallization of one of the blend components forces the separation of components. The modification of transport processes may cause an increase as well as a decrease of the energy barrier depending on the properties of the second blend component, whereas the substitution of Δg_f by $\Delta g_f'$ always increases the energy bar-

rier for critical nucleus formation (the sign of Δg_m is negative).

It follows from Eq. (6) that the ratio I/G does not depend on the transport term, so when homogeneous nucleation dominates in the primary nucleation process, the changes in the average spherulite radius in the blend compared to plain iPP should result from the increase of the energy barrier for the formation of the critical size nucleus. It may be expected that in the absence of other phenomena the average radius of spherulites crystallized from miscible or partially miscible systems should be greater than in a plain crystallizing polymer. Such behavior was found experimentally for a miscible system of iPP with atactic polypropylene (aPP).¹⁴ However, Figure 6 shows that iPP/iPB blends exhibit another dependence of the average spherulite radius on the crystallization temperature. At $T_c > 80^\circ\text{C}$, where the heterogeneous nucleation controls the average spherulite radius, R^* in blends is greater than in plain iPP, which indicates that the number of heterogeneous nuclei decreases in blends with increasing content of iPB, similar to low undercooling. The densities of heterogeneous primary nucleation at T_c above 80°C (as calculated per iPP volume unit present in the blend) equal 1×10^9 nuclei/cm³ for plain iPP, 6×10^8 nuclei/cm³ for the 9 : 1 iPP/iPB blend, and 4.7×10^8 nuclei/cm³ for the 7 : 3 blend. However, with the decrease of T_c the radii of spherulites in the blends decrease faster than in plain iPP, and finally at T_c below 74°C the average spherulite radius in the blends becomes smaller than in plain iPP. This is contrary to what was expected on the basis of considerations of component segregation upon crystallization.

A reasonable fit of the experimental dependence of average spherulite radius on crystallization temperature of the iPP/iPB blends could be obtained only under the assumption of a strong temperature dependence of free enthalpy of mixing Δg_m . Such an assumption is, however, very unrealistic. Thus,

it is concluded that another phenomenon influences the number of spherulites in the blends. In our opinion this is the crystallization of iPB component near 70°C . Gohil and Peterman¹⁰ reported that during nonisothermal crystallization of iPP/iPB blends, with a cooling rate of $10^\circ\text{C}/\text{min}$, the crystallization of iPB proceeds at the temperature near 70°C . Melt crystallized isotactic poly(butene-1) forms spherulites, similar to iPP. Since the undercooling for iPP is extremely high, even a slight change of energetic conditions can result in the formation of additional iPP nuclei: interfaces of iPB crystals with iPP melt may induce additional nucleation of iPP. In that way two additional fractions of spherulites can appear in the blend: small iPB spherulites nucleated inside iPB-rich inclusions and iPP spherulites nucleated on the interfaces.

In order to determine the temperature range of fast crystallization of iPB, studies of nonisothermal crystallization of the blend were carried out. The samples of 7 : 3 iPP/iPB blend were crystallized from the melt in the DSC cell with various cooling rates and temperatures of maximum crystallization rate were determined. The results are presented in Table II. Extrapolation to the zero-cooling rate (the case of isothermal crystallization) gave a value in the range of $77\text{--}78^\circ\text{C}$. This value is in a good agreement with the temperature at which the nucleation process in iPP/iPB blends becomes more intensive than the crystallization of plain iPP (see Fig. 6). In our opinion the crystallization of iPB, sufficiently fast at that temperature, causes the formation of a new fraction of iPB and iPP spherulites, which influences the average radius of spherulites stronger than the possible decrease of homogeneous primary nucleation rate of iPP due to segregation of iPB. Consequently, the average spherulite radius in blends is lower than that in plain iPP. However, the light-scattering method is unable to distinguish between the contribution of iPP and iPB spherulites. Due to different polarizabilities of the iPB and iPP crystallites the iPB spherulites may influence the SALS pattern with different weight than iPP spherulites, which in turn can modify the average radius of spherulites estimated on the basis of such a pattern.

On the basis of the above considerations the following picture emerges: at all T_c the rate of homogeneous nucleation in the blends is slightly lower than that in plain iPP crystallized at the same temperature as a consequence of a separation of blend components occurring during crystallization. A decrease in the homogeneous nucleation rate is masked

Table II Peak Temperatures of Nonisothermal Crystallization of 7 : 3 iPP/iPB Blend for Various Cooling Rates

	20 °C/min	10 °C/min	5 °C/min	2.5 °C/min	1.25 °C/min
iPP peak	107.5	112	116	119	122.5
iPB peak	69	70	71.5	73.5	75.5

by the formation of iPB spherulites followed by nucleation of additional iPP spherulites at iPB spherulite interfaces, except for a narrow range of 77–80°C. The average radius of spherulites in the blends is then a result of a superposition of those processes. Above 80°C the average radius is controlled by the heterogeneous nucleation of iPP, which is slightly depressed by the presence of iPB in the blend due to an increase of the barrier for critical nucleus formation, similar to homogeneous nucleation.

CONCLUSIONS

The results reported here show that iPP and iPB are miscible but show a phase separation when annealed at elevated temperature. The melt annealing of iPP/iPB blends causes the partial separation of the components and formation of two-phase morphology: iPB-rich inclusions dispersed in iPP-rich matrix. The efficiency of the phase separation and actual composition of the inclusions and the matrix depend on temperature and/or time of the annealing process.

It was found that both heterogeneous and homogeneous primary nucleation modes of iPP spherulites in the iPP/iPB blends are influenced by the presence of iPB. At low undercooling, at which only the heterogeneous mode of nucleation is active, the number of primary nuclei per volume unit of iPP in the blend decreases slightly with the increase of iPB concentration. This decrease is more pronounced for high undercoolings. It was also found that the activity of the less active heterogeneities is more strongly depressed than those that are highly active.

The rate of homogeneous nucleation of iPP also decreases with increasing iPB content in the blend since the crystallization of iPP evokes complete separation of partially miscible components and the energy barrier for the formation of a critical size nucleus is increased.

At very low crystallization temperature (below 77°C), the crystallization of iPB in the blends proceeds simultaneously with iPP crystallization. This causes the lowering of the average spherulite radius in the blends due to the formation of a number of iPB spherulites and the nucleation of an additional fraction of iPP spherulites on interfaces with iPB crystallites.

REFERENCES

1. J. L. Way and J. R. Atkinson, *J. Mater. Sci.*, **7**, 1345 (1972).
2. A. Galeski, Z. Bartczak, and M. Pracella, *Polymer*, **25**, 1323 (1984).
3. Z. Bartczak, A. Galeski, and M. Pracella, *Polymer*, **27**, 537 (1986).
4. Z. Bartczak, A. Galeski, E. Martuscelli, and H. Janik, *Polymer*, **26**, 1843 (1985).
5. Z. Bartczak, A. Galeski, and N. P. Krasnikova, *Polymer*, **28**, 1627 (1987).
6. A. J. Foglia, *Appl. Polym. Symp.*, **11**, 1 (1969).
7. A. Pilo, J. Y. Decroix, and J. F. May, *Angew. Makromol. Chem.*, **54**, 77 (1976).
8. A. Siegman, *J. Appl. Polym. Sci.*, **24**, 2333 (1979).
9. M. Canetti, A. M. Bonfatti, P. Sadocco, A. Seves, and M. Pracella, *Polym. Network Blends*, **3**, 83 (1993).
10. R. M. Gohil and J. Peterman, *J. Macromol. Sci.-Phys.*, **B18**, 217 (1980).
11. J. Boor and J. C. Mitchell, *J. Polym. Sci.*, **62**, S70 (1962).
12. A. M. Freedman, D. C. Basset, and R. H. Olley, *J. Macromol. Sci.-Phys.*, **B27**, 319 (1988).
13. M. Pluta and M. Kryszewski, *Acta Polym.*, **37**, 727 (1986).
14. Z. Bartczak and A. Galeski, *Polymer*, **31**, 2027 (1990).
15. B. Wunderlich, *Macromolecular Physics*, Vol. 2, Academic Press, New York 1976.
16. R. D. Icenogle, *J. Polym. Sci. Polym. Phys. Ed.*, **23**, 1369 (1985).
17. A. Galeski, *J. Polym. Sci. Polym. Phys. Ed.*, **19**, 721 (1980).
18. A. Galeski and E. Piorkowska, *J. Polym. Sci. Polym. Phys. Ed.*, **19**, 731 (1980).
19. J. R. Burns and D. Turnbull, *J. Appl. Phys.*, **37**, 4021 (1966).
20. J. A. Koutsky, A. G. Walton, and E. Baer, *J. Appl. Phys.*, **38**, 1832 (1967).
21. R. S. Stein and M. B. Rhodes, *J. Appl. Phys.*, **31**, 1873 (1960).
22. E. Piorkowska and A. Galeski, *J. Polym. Sci. Polym. Phys. Ed.*, **23**, 1723 (1985).
23. J. D. Hoffman, in *Treatise on Solid State Chemistry*, Vol. 3, N. B. Hannay, Ed., Plenum Press, New York, 1976, Chapter 7.
24. E. J. Clark and J. D. Hoffman, *Macromolecules*, **17**, 878 (1984).

Received February 23, 1994

Accepted June 6, 1994